FERMILAB-LU-112

Evolution of the 400 MeV Linac Design

James A. MacLachlan

9 November 1987

Abstract

The basic premises of the conceptual design for the linac upgrade[1] are pursued to establish lengths, gradients, power dissipation, *etc.* for the 400 MeV linac and matching section. The discussion is limited to accelerating and focusing components. Wherever values depend on the choice of the accelerating structure, the disk-and-washer structure is emphasised; the results are generally relevent to the side coupled cavity choice also.

1 Introduction

In April, 1987, the Fermilab linac group released a conceptual design[1] for an upgrade of the existing linac replacing 200 MHz tanks 6–9 (116–200 MeV) with higher gradient 805 MHz sections to reach 400 MeV in the same space. A major goal of the conceptual design was to establish a credible cost estimate based on the side-coupled cavity (SCC) structure of the Los Alamos LAMPF linac. The report also discusses the disk-and-washer (DAW) structure as an attractive alternative which is less fully developed in the parameter range of interest to Fermilab. In the following six months the linac group started calculations for both types of structure to optimise power consumption, effective accelerating field, and peak surface field throughout the energy range.[2] These calculations are sufficiently advanced to permit reasonably concrete description of the linac itself; the details of rf power sources, fabrication procedures, and mechanical systems are also better known but not treated here. The Los Alamos work provides a good understanding of what can be expected from the SCC.[3] There is also considerable known about the DAW.[4] Both calculations and hardware development at Fermilab have so far emphasised the DAW because of its apparent advantages. The object is to evaluate, and so far as necessary, find

[1] *Tevatron Upgrade — Linac Conceptual Design*, Fermilab, April 1987

[2] Initally, Al Moretti, principally Leroy Leary for the DAW structure, and more recently Tom Jurgens for the SCC structure.

[3] *e.g.*, E. A. Knapp *et al.*, Rev. Sci. Inst.,39 no. 7(7/68)

[4] R. K. Cooper *et al.*, Radio-Frequency Structure Development for the Los Alamos/NBS Racetrack Microtron, LA-UR-83-95, Los Alamos Natl. Lab(1/83) and references cited therein

remedies for the problems that have limited the application of DAW to date. Because this report considers primarily the questions of length, strength, and power dissipation of accelerating and focusing elements it does not bear crucially on the choice of structure except as it reflects the higher expected shunt impedance of DAW. Where the properties of a particular rf structure are relevent DAW is featured, but most of the conclusions apply at least in general to either structure.

2 200 MeV Beam Properties

Table 1 collects important properties of the 116 MeV H^- beam at the end of tank 5 of the 200 MHz Alvarez linac. It also serves to define some symbols used in later remarks. The entries are based on a combination of measurements at 750 keV and PARMILA calculation[5] using the best available information on tanks 1–5. Unfortunately, there is insufficient space in the existing linac structure to measure beam properties at 116 MeV. Therefore, the design can not be tied too closely to properties of the input beam.

Kinetic energy (T)	116.54	MeV
ε_L (90 %, invariant)	6.2 $\times 10^{-5}\pi$	eVs
ε_T (90 %, unnormalised)	10. π	mm mrad
Beam current, averaged over pulse (I_b)	50.	mA
Tank 5 frequency (f)	201.25	MHz
Effective tank 5 gradient (E_0T)	1.82	MV/m
Tank 5 accelerating phase (φ_s)	-32.	deg

Table 1: 116 MeV Beam Parameters

Because the rf frequencies of the old and new parts of the linac differ, a transition section for matching bunch length and momentum spread is required between them. This section also must be specified to provide for transverse matching with sufficient flexibility to accommodate both operating variability and the current incomplete knowledge of the incoming beam. Although one could to some degree adjust 200 MHz tank 5 to match the beam to the new sections, bunch matching will in any case be required. It will be seen that provision for flexible matching does not significantly complicate the design; therefore tank 5 can be setup for optimum performance without regard for requirements of the new structure. The more important numbers in Table 1 are the energy, emittances, and intensity of the beam. The calculated beam ellipse parameters

[5] Elliot McCrory, priv. comm.

are used for specificity; they are considerably different from what one would expect for a beam matched to the existing linac.

3 Design Assumptions and Criteria

The removal of tanks 6–9 frees 66 m for linac, matching section, and necessary changes to the downstream transport line. Therefore, one wants a net acceleration $E_0T\cos\varphi_s$ of about 4 MV/m, considerably higher than that at any operating proton linac. The surface gradient at which a structure will spark is approximately proportional to the square root of the frequency. The relation has been expressed[6] in the form

$$f = 1.643E_K^2 e^{-8.5/E_K}$$

where f is the frequency in MHs and E_K is the sparking limit in MV/m, the "Kilpatrick limit". At 805 MHs E_K is about 26 MV/m. The numerical coeficient in the equation for the limit is sensitive to vacuum and surface conditions. In current practice a factor variously quoted as 2–3 times E_K is regarded as being sustainable in routine operation. Furthermore, for systems excited with pulses shorter than one millisecond the threshold is higher than for cw operation. From these considerations and a survey of the literature on voltage breakdown in vacuum, a multiplier of 1.6 has been applied to the Kilpatrick limit.[7] This value permits installing the new linac in the available space and is nonetheless conservative.

The SCC structure is illustrated in Fig. 1. Between two accelerating sections is shown an offset rf coupler, called a bridge coupler, which is a suitable place to excite the structure and can pass the rf around a focusing quad. To maintain synchronism between the rf and beam particles these couplers must have length equal to an odd multiple of the elementary cell length $\beta\lambda/2$. In this expression β is the particle velocity divided by the speed of light and λ is the free space wavelength of the rf. Figure 1 is drawn for the case of a three-cell coupler, but if single-cell couplers can be made to serve adequately they are to be preferred for the space saving and the simplicity of the rf design. It will be shown later that the required transverse focusing can be accommodated in a one-cell coupler; it is assumed that an 800 MHs wave guide can be matched into one. The DAW structure is shown in Fig. 2. Here also the fundamental cells have length $\beta\lambda/2$; a single-cell coaxial coupler is shown. The coaxial geometry follows naturally from the basic structure.

The starting point for the design to be described is given by the conceptual design. Table 2 collects the parameters assumed. In Fig. 3 the effective accelerating gradients E_0T for SCC structure derived from the LAMPF linac and for DAW structure are plotted as functions of β with ordinates on the lefthand

[6] W. D. Kilpatrick, Rev. Sci. Inst. 28,p824(1957)
[7] R. Nobel, Fermilab TM - 1448, unpub.

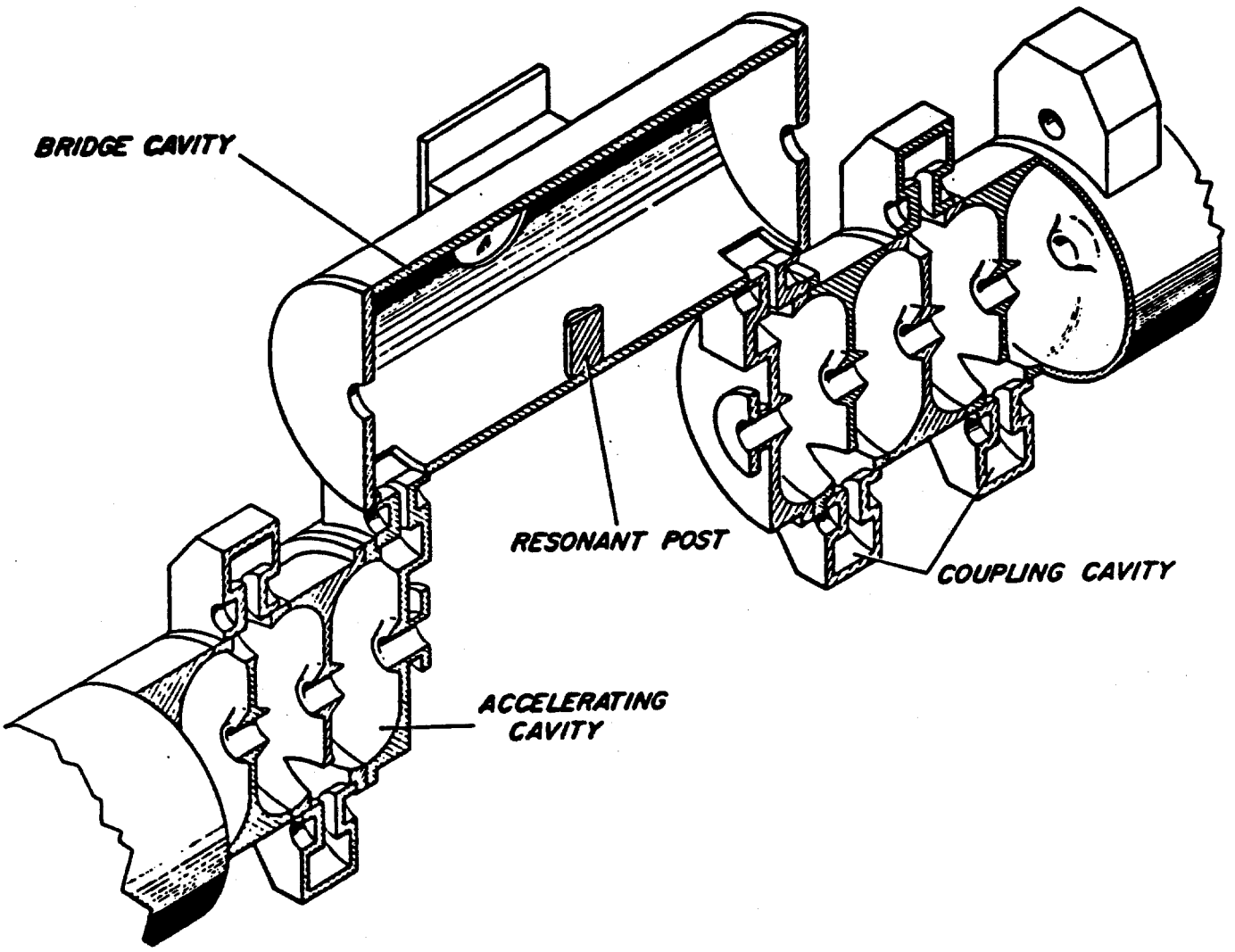

Figure 1: Side-coupled cavity structure and $\frac{3}{2}\beta\lambda$ bridge coupler (after E. A. Knapp in *Linear Accelerators*,Lapostolle and Septier,*ed.*,p615,North Holland(1970)

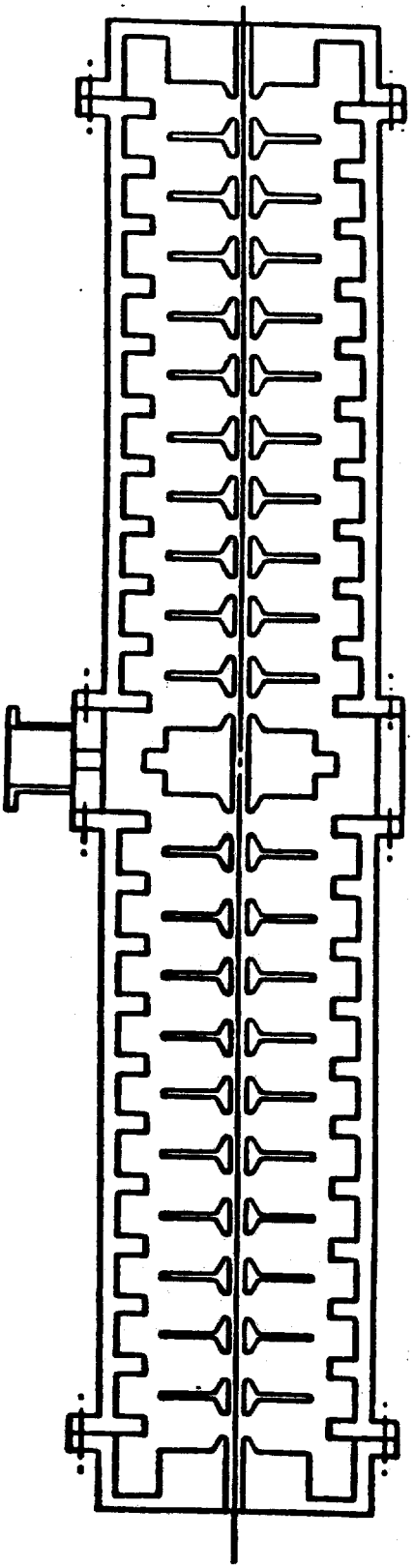

Figure 2: Disk-and-washer structure and $\beta\lambda/2$ coaxial coupler (after a sketch of the LASL PIGMI proposal)

Frequency of rf (f)	805.0	MHz
Maximum surface field ($E_m, 1.6E_K$)	42.	MV/m
Accelerating phase (φ_s)	-32.	degree
Length	$< 55.$	m
Number of modules	7	
RF power/module	$\sim$10.	MW
RF pulse length	$< 100.$	μs
Repetition rate	15.0	Hz
Beampipe radius (r_p)	1.5	cm
Quadrupole poletip radius (r_q)	2.0	cm

Table 2: Design Assumptions

axis. The continous curves are third order least squares fits. Also plotted with ordinates referred to the righthand axis are the power dissipation per meter for each structure when excited to give a maximum surface field of 42 MV/m. Both structures were calculated to strictly maximise the shunt impedance per meter Z_{sh}. There is evidence that the apparent deficiency of SCC in peak field at high β can be eliminated with insignificant reduction in Z_{sh} by increasing the accelerating gap slightly. A set of such calculations for the full range of β is not yet complete. However, neglecting the expectation that the two structures will be degraded from calculated Z_{sh} by differing amounts because of differences in fabrication, coupling ports (SCC), support T's (DAW), *etc.*, the current information favors DAW because of its higher Z_{sh}. No adjustment has been made to the Z_{sh} calculated by SUPERFISH in this note. Such an adjustment is expected from Los Alamos experience to be $\sim$ 15% for both structures, but information for DAW is less complete.

When the DAW is excited to E_m at all β, the dissipation is approximately constant at 1 MW/m whereas the effective accelerating gradient increases with increasing β. For the present optimisation of the SCC, however, the attainable gradient is roughly constant while the power/m drops. This qualitative difference leads to different optima for the distribution of the cells among the modules; both patterns of distribution are treated in the next section. If one modifies the SCC parameters to give the same ratio of E_0/E_m then the segmentation into rf power modules and sections for transverse focusing will depend on the choice of rf structure primarily through differences in Z_{sh} and the relative advantages of the two types of coupler. Both three dimensional field calculations and hardware R&D are are expected to contribute to the determination of the physically realisable shunt impedance. The available information on such additional considerations as mode spectrum,[8] fabrication, operational properties,

[8]Deflecting modes are no problem for 100 MeV protons. F. Mills & R. Nobel, priv. comm.

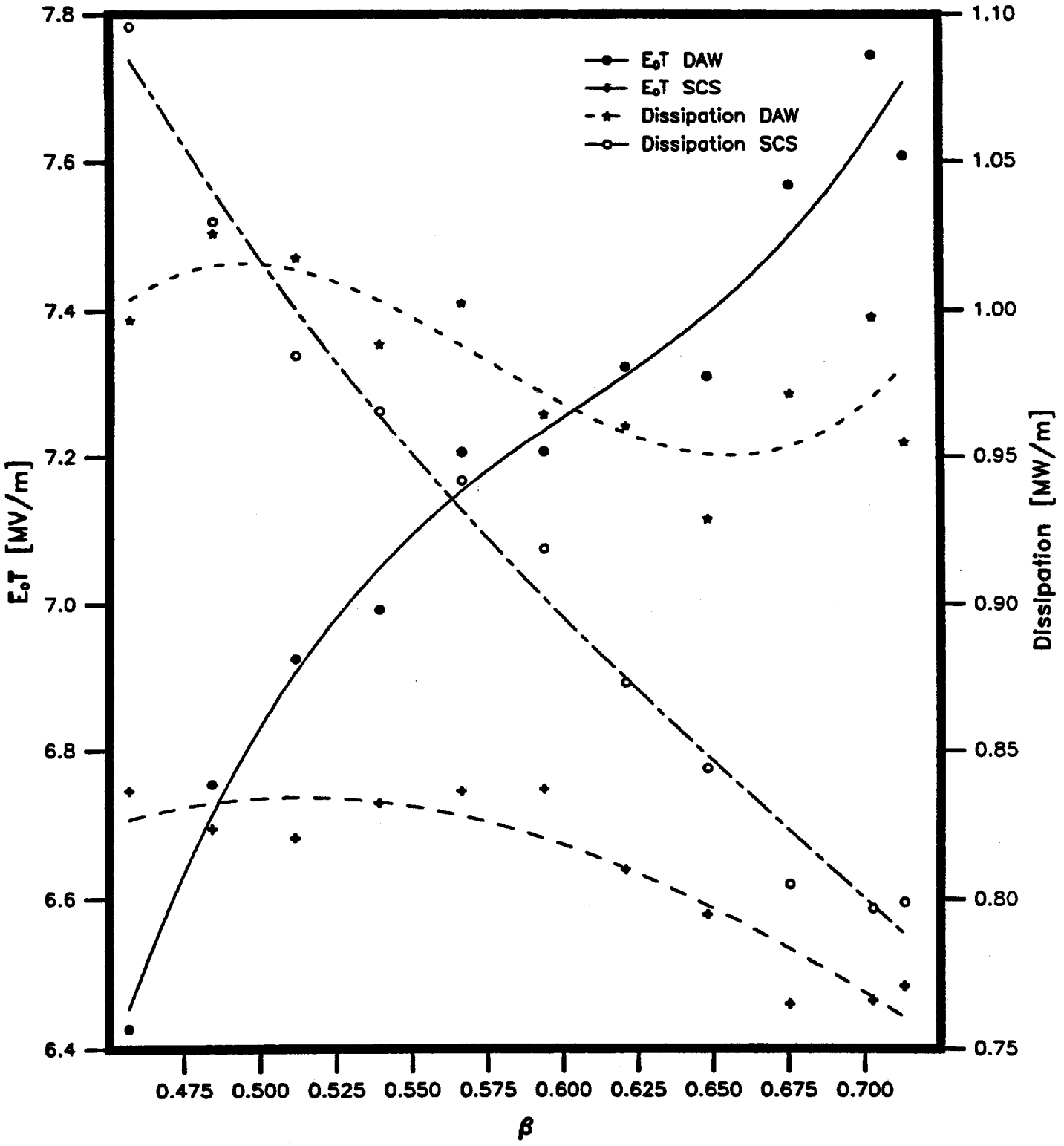

Figure 3: Third order least squares fits to effective accelerating gradient E_0T and power dissipation per meter for $E_{max} = 42$ MV/m for both DAW and SCC as functions of β

etc. does not clearly dictate the choice of either structure. Both calculations and measurements in progress are expected to allow an unequivical choice. The details of DAW optimisation including parameter dependencies of Z_{sh}, average axial field E_0, and transit time factor T will be covered in a future TM.[9]

4 Segmentation

The motivation for the assumed number of rf modules is an expected Z_{sh} about 50 MΩ/m and a perception that the most economical klystron rf generator would provide about 10 MW. For DAW the β-dependance of the dissipation indicates that the modules should all have about the same length, 7–8 m. Uniform distribution of the rf power favors feeding the modules from the center, so there will be a coupler at that location which can accommodate a quad also. It will be shown that the rf defocusing requires that the quads of a FODO channel be < 2 m apart in the first modules. Symmetry with respect to the rf feed point requires an even number of sections per module, so either four or six sections can be considered for FODO focusing and possibly two sections if multiplets are used. The focusing scheme and options will be treated more fully in the next section, but the present preferred scheme, a subdivision of each module into six accelerating sections with FODO focusing, is discussed here. If hardware development demonstrates that the current plans are too optimistic with respect to Z_{sh} or the power of the most economical klystron, the consequence of the ideas that have been used in this note would be to be to go to eight modules, most likely with four FODO sections each.

The required number of accelerating gaps and the manner of dividing them up between modules is determined from the structure calculation in a several-step iteration. Denote by R the ratio of the maximum surface field E_m to the average axial field E_0. $R(\beta)$ is known from the SUPERFISH results. The number of accelerating gaps required to raise the energy from 116 MeV to 400 MeV is calculated subject to the condition $E_m = 42$ kV/m in every cell from $R(\beta)$, $T(\beta)$, and $Z_{sh}(\beta)$ as represented by the third order fits obtained for DAW. The cells are then divided into seven groups of equal dissipation including loading from 50 mA beam current. Figure 4 shows a plot of kinetic energy and power/m as a function of cell number. Each of the seven modules is divided into six equal sections. The cell count in a module is adjusted to the nearest odd multiple of six. The multiple must be odd because the basic structural assembly of the DAW is made up of two washers with their common T-support as shown in Fig. 2, and the termination provided by either a module end or a coupler is an additional half accelerating cell at each end of a section. The acceleration is then recalculated iteratively to determine a constant cell length $\bar{\beta}\lambda/2$ where $\bar{\beta}$ is the β corresponding to the average energy in the section for a particle that

[9] L. Larry, in preparation

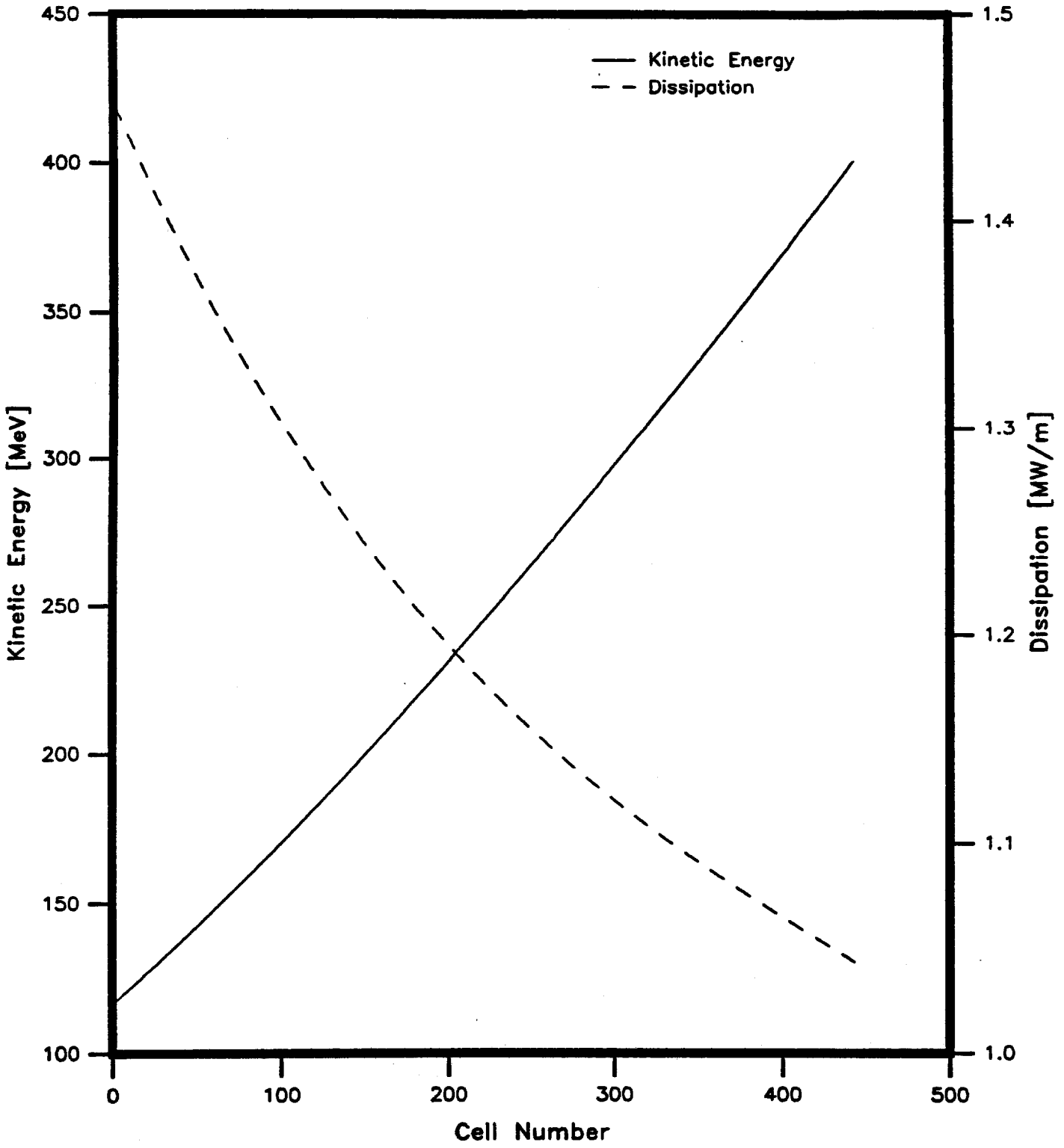

Figure 4: Kinetic energy and power dissipation per meter as functions of cell number

Module Number	T [MeV]	E_0 [MV]	Number of Cells	Length [m]	Power [MW]
1	155.7	7.12	6×13	7.596	8.51
2	194.6	7.70	6×11	7.204	8.37
3	236.2	7.70	6×11	7.789	8.51
4	275.3	8.46	6× 9	6.902	8.28
5	315.9	8.46	6× 9	7.250	8.35
6	357.7	8.46	6× 9	7.560	8.40
7	400.5	8.46	6× 9	7.838	8.40
Totals			426	52.272	58.81

Table 3: Segmentation of DAW Linac

enters and leaves the section with the correct phase.[10] The number of cells in higher energy modules is less than in the lower energy modules. The average axial field E_0 is adjusted slightly by requiring that each module dissipate the same power. Table 3 summarises cell number, gradient, energy, *etc.* for each module. Table 4 is a similar result using the β-dependance of parameters for SCC. In this case the modules are subdivided into four sections because the power distribution leads to shortrer modules at the lowenergy end. This option is developed more fully in the following section.

5 Transverse Focusing

The rf power distribution scheme results in a symmetric arrangement of accelerating sections with a coupler at the midpoint. The further segmentation required to provide for transverse focusing can be established by calculation of the growth of the beam envelope from a waist in the structure to a proposed quad location. The rf defocusing has its greatest strength relative to the focusing quads at the low energy end of the linac where the unnormalised transverse emittance is also highest. Furthermore, there is more transverse tune spread arising from the bunch width, ± 20 deg at injection. The space charge contribution, also strongest at low energy, is only a detail because the tune depresion is $\sim 10\%$. For this reason one determines the appropriate spacing in module 1 and then uses that result plus considerations of periodicity, segmentation, modularity, and adiabatic scaling of parameters to establish the overall focusing scheme.

[10] Two computer programs have been written for these calculations. The first calculates the number of cells with independent $\beta\lambda$ required; the second calculates $\bar{\beta}\lambda$ and energy gain for the segmented structure.

Module Number	T [MeV]	E_0 [MV]	Number of Cells	Length [m]	Power [MW]
1	151.5	8.82	4×14	6.100	8.95
2	189.0	8.59	4×14	6.696	9.02
3	228.1	8.34	4×14	7.231	9.01
4	268.7	8.15	4×14	7.712	9.06
5	310.3	7.97	4×14	8.143	9.05
6	353.1	7.85	4×14	8.529	9.13
7	396.4	7.67	4×14	8.873	9.03
Totals			392	53.284	63.26

Table 4: Segmentation of SCC Linac

For each choice of quad spacing there is a particular $\check{\beta}$, the width Twiss parameter at the waist, for which $\hat{\beta}$ at the quad has its minimum value.[11] If one can arrange a sufficiently regular placement of the quads, the values $\hat{\beta}$ and $\check{\beta}$ can be used as fitting conditions at all the beam waists along the structure to determine the required quad strengths. However, the segmentation determined by power distribution for DAW results in a non-monotonic set of module lengths. Thus, the best control of the beam envelope can be obtained by using different characteristic β's for each value of the number of cells per section. A relatively easy way to arrive at *some* solution is to scale the β values matched to module 1 to the average module length and apply this pair as fitting conditions throughout. As illustrated in Fig. 5 the resulting beam envelope is probably as good as needed practically; a more polished result could come from complete matching at each location where the number of cells per section is changed. Table 5 gives the calculated quad strengths and the phase advance per focusing cell.

The quads used in the FODO focused DAW linac are all the same, *i.e.*, at 8 cm magnetic length short enough to fit into the shortest $\beta\lambda/2$ coupler. The poletip fields given in Table 5 all appear manageable in an electromagnetic quad. It may nonetheless be advantageous to use some PMQ's for reasons other than their high gradient capability. There may be useful simplification of the mechanical structure by elimination of the power and water requirements and valuable operational simplification by eliminating some pulsed power supplies which are subject to both failure and mis-seting. Some adjustable quads will of course be required to accommodate changes in operating conditions, and the locations between modules appear to be the most accesible spots. Because

[11] The minimax $\hat{\beta}$ is easily found in a few trials. In this work the program TRACE3D written by K. R. Crandall, then at Los Alamos, was used.

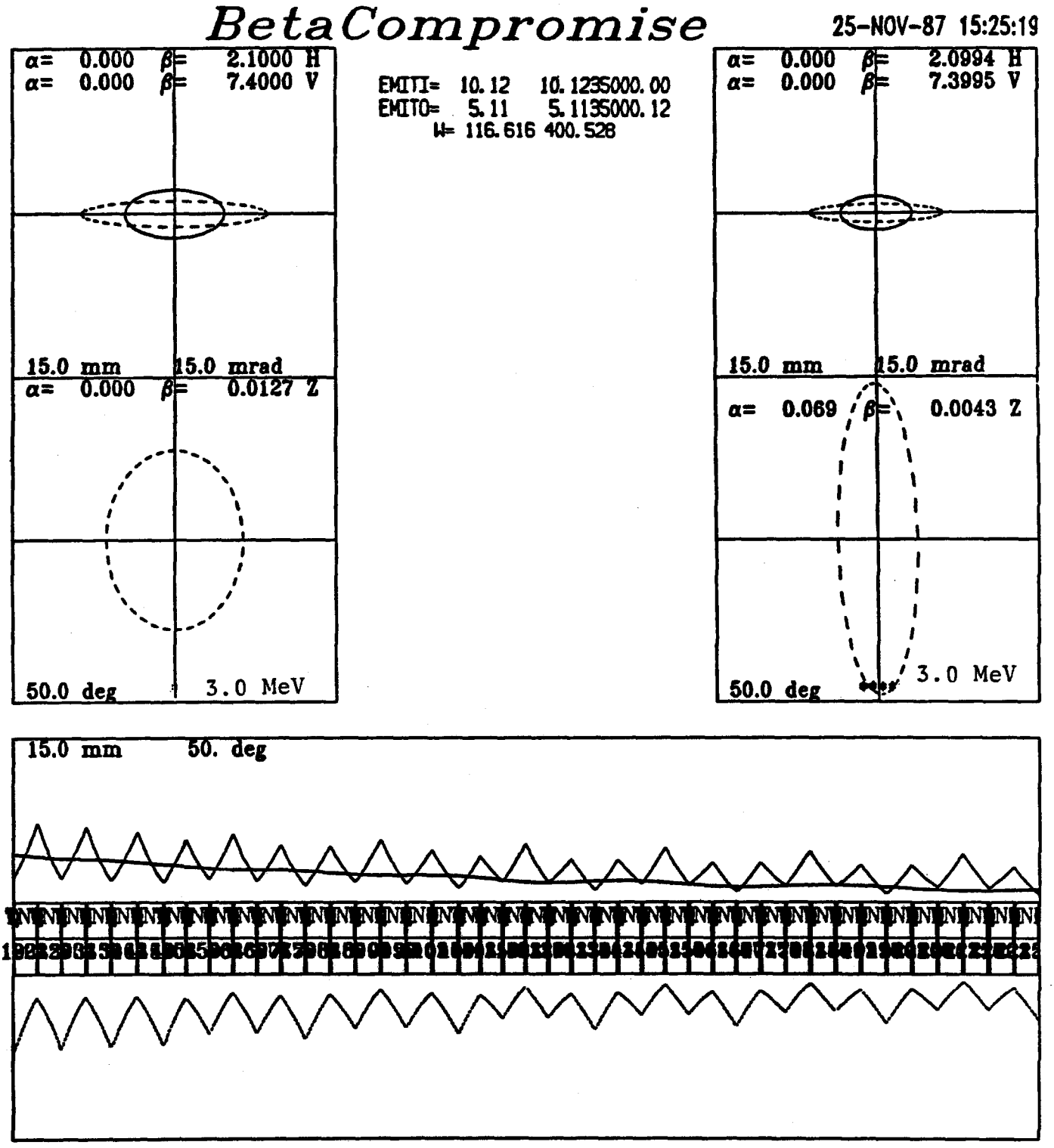

Figure 5: Beam envelopes for the DAW linac computed by TRACE3D using matching β's scaled by the average length of all modules from those matched to module 1

Modules	Quad Poletip Fields Sections 1	2	3	4	5	6	Avg Phase Advance per Cell
1	-4.14	4.16	-4.32	4.45	-4.20	4.19	41.3
2	-4.34	4.31	-4.29	4.48	-4.33	4.32	39.0
3	-4.51	4.37	-4.36	4.55	-4.42	4.42	42.3
4	-4.75	4.48	-4.48	4.96	-4.55	4.54	36.7
5	-5.02	4.60	-4.59	5.08	-4.67	4.67	38.3
6	-5.15	4.73	-4.74	5.21	-4.80	4.81	40.5
7	-5.28	4.88	-4.90	5.36	-4.97	4.98	41.5

Table 5: Quad poletip fields [kG] and transverse oscillation phase advance per focusing cell [deg] for the FODO Focused DAW Linac

of symmetry about the center coupler, the quad there should be adjustable also to provide alternation of adjustable quad polarities. If the mechanical design places a premium on space between the modules because of flanges, vacuum valves, BPM's, *etc.*, then one could place PMQ's at the ends and center and conventional quads elsewhere. The optics described are suitable for either arrangement.

Figure 6 shows a beam envelope plot calculated from parameters for the SCC. Because the optimum power distribution leads to a fixed number of cells per section, the section lengths increase smoothly with energy. Because the low energy modules are shorter only four sections per module are required to get the required quad spacing at low energy. The very smooth behavior of the beam envelope is obtained using a single $\hat{\beta}, \bar{\beta}$ pair for the focusing conditions. Unfortunately, this pleasing situation from the standpoint of simple transverse optics results from an undesirable limitation on accelerating gradient which yields in turn a longer structure.

The possibility of using quad doublets or triplets instead of the FODO scheme has been examined. Because couplers dissipate some rf power and take up scarce space there is appeal to the idea of reducing the number of couplers by focusing in both planes at each break in the accelerating structure. However, the beam spreads too fast to be contained by multiplets only between modules. Therefore, the center coupler must contain a multiplet. For a doublet the coupler must be at least $\frac{2}{3}\beta\lambda$ long and for a triplet at least $\frac{5}{3}\beta\lambda$. Thus, compared to four-section FODO modules there is no space saving from using doublets and a loss from triplets; compared to six-section FODO modules doublets save some space, but triplets do not. Much stronger quads are needed in closely spaced multiplets than in FODO cells. If electromagnet quads are to be used in the couplers, additional problems of cooling and magnet design are raised.

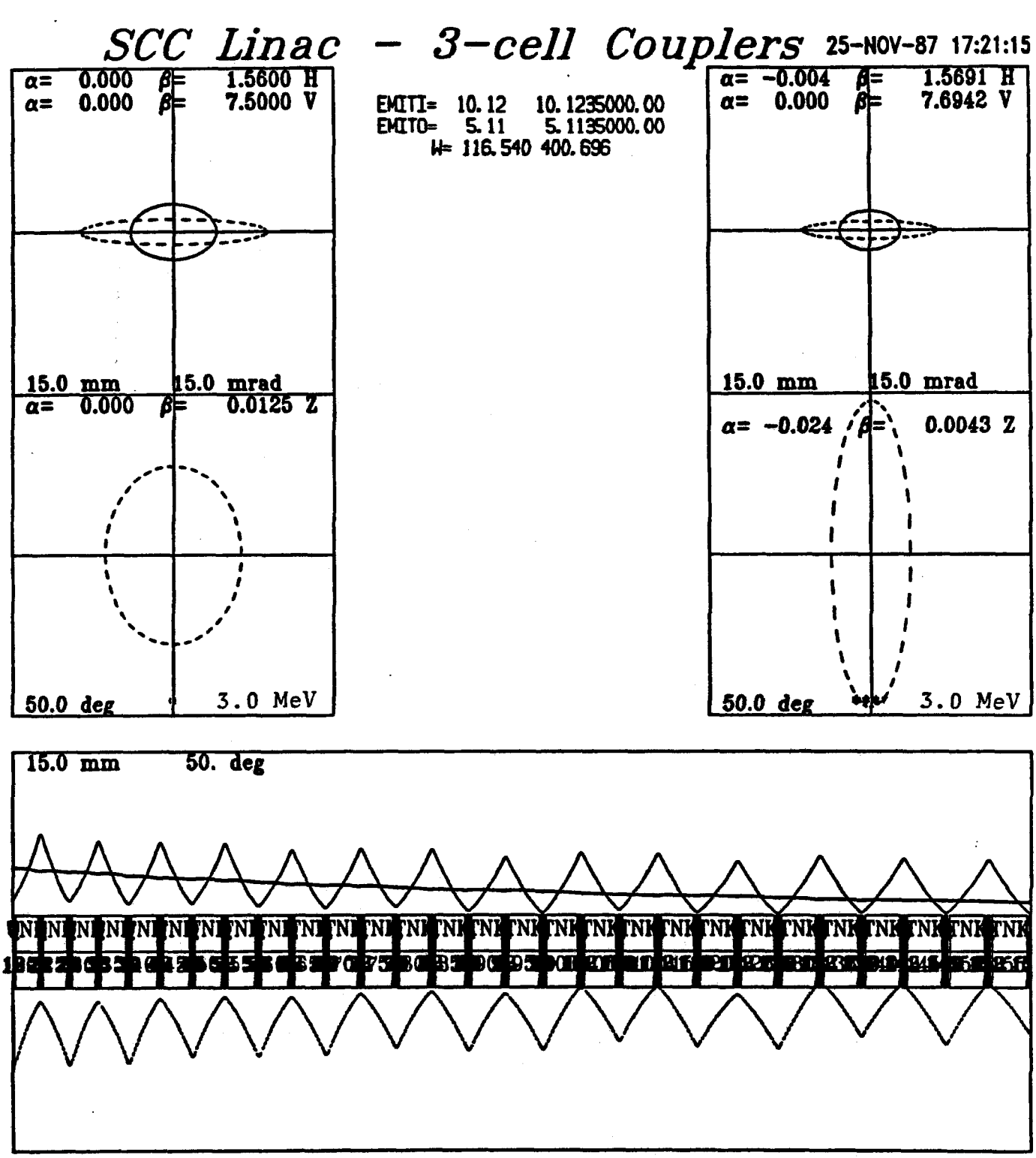

Figure 6: Beam envelopes for SCC FODO-focused linac with four accelerating sections per module

The stigmatic focusing of doublets plus the more critical setting tolerance would probably complicate routine tuning considerably. The beam can usually find its way through a FODO channel even if the gradients are set very crudely. The tuning and matching properties of a symmetric triplet scheme seem more tidy, but settings are nonetheless critical. The greater length devoted to focusing components argues against it.

There is one version of the doublet scheme that retains appeal as an alternative if the couplers, as yet not fully designed, prove unexpectedly lossy or otherwise undesirable. In this variant the inter-module doublets are electromagnetic but those in the center couplers might be PMQ's. If the focuing polarities are alternated with mirror symmetry, *e. g.* DoFOFoDODoF where "o" is a short drift and "O" contains the rf structure, then at the centers of the o's $\beta_x = \beta_y$ and $\alpha_x = \pm\alpha_y$. Figure 7 shows beam profile plots for module 1 as a single doublet cell with two sections of ~ 2.8 m separated by a $\frac{3}{4}\beta\lambda$ coupler, a pattern which can be repeated for six more modules. This result illustrates the general character of the solution and establishes the required quad strength. For 8 cm quads of 2 cm bore radius the pole tip fields are in the range 10–12 kG; the design of such a doublet is marginal even for PMQ's.

6 Electromagnetic Quadrupoles

The length of a $\beta\lambda/2$ coupler at 116 MeV is ~ 8.5 cm; therefore at the low energy end, at least, suitable quads must be rather compact. To be certain that the desired parameters are reasonable, the first steps of the electrical design have been carried out. The aim has been to procede sufficiently far to establish the field quality, electrical parameters, and approximate mechanical properties. Figure 8 shows the conceptual design for a crossection of an octant. The coil window is filled by two twelve-turn coils for each pole, excited in parallel. It has been sized to contain copper enough that no direct cooling of the coil should be required for pulsed operation at maximum design gradient. The poles should be excited with a parallel current feed to reduce the inductance. This slight complication is probably preferable to the additional requirements for turn-to-turn and coil-to-core insulation for four times the $L\frac{dI}{dt}$ voltage. Calculated magnetic field properties and estimated electrical properties are given in Table 6. The saturation curve used is the default in the POISON program; eddy current effects have not been calculated.

7 Transition Section

The transition section is required to transform the bunch width and momentum spread from the existing linac to that matching the stronger longitudinal focusing in the high gradient structure. It also provides for transverse matching from short to longer focusing cells. The last cell in tank 5 of the

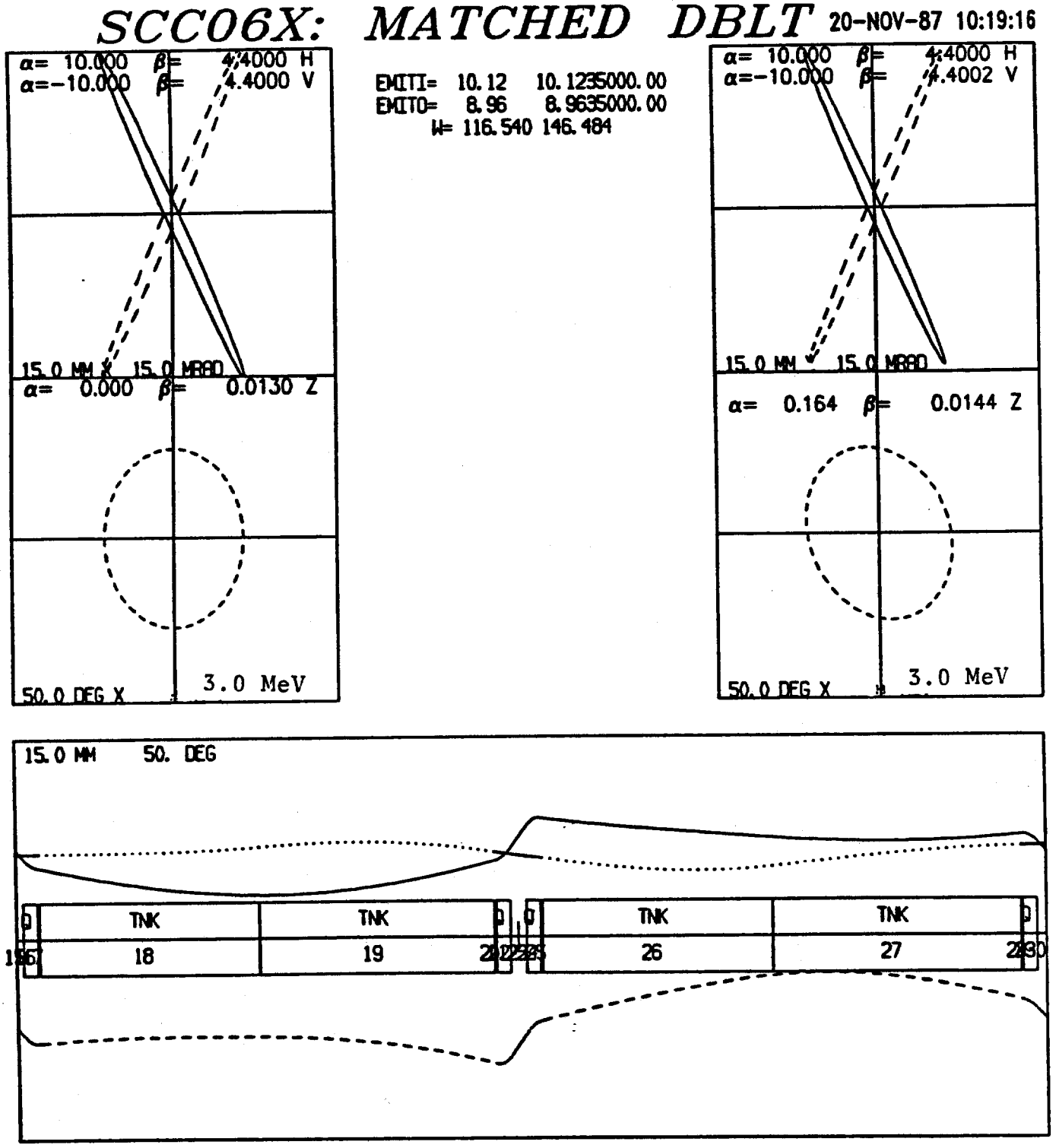

Figure 7: Beam envelopes for module 1 as a doublet focusing cell

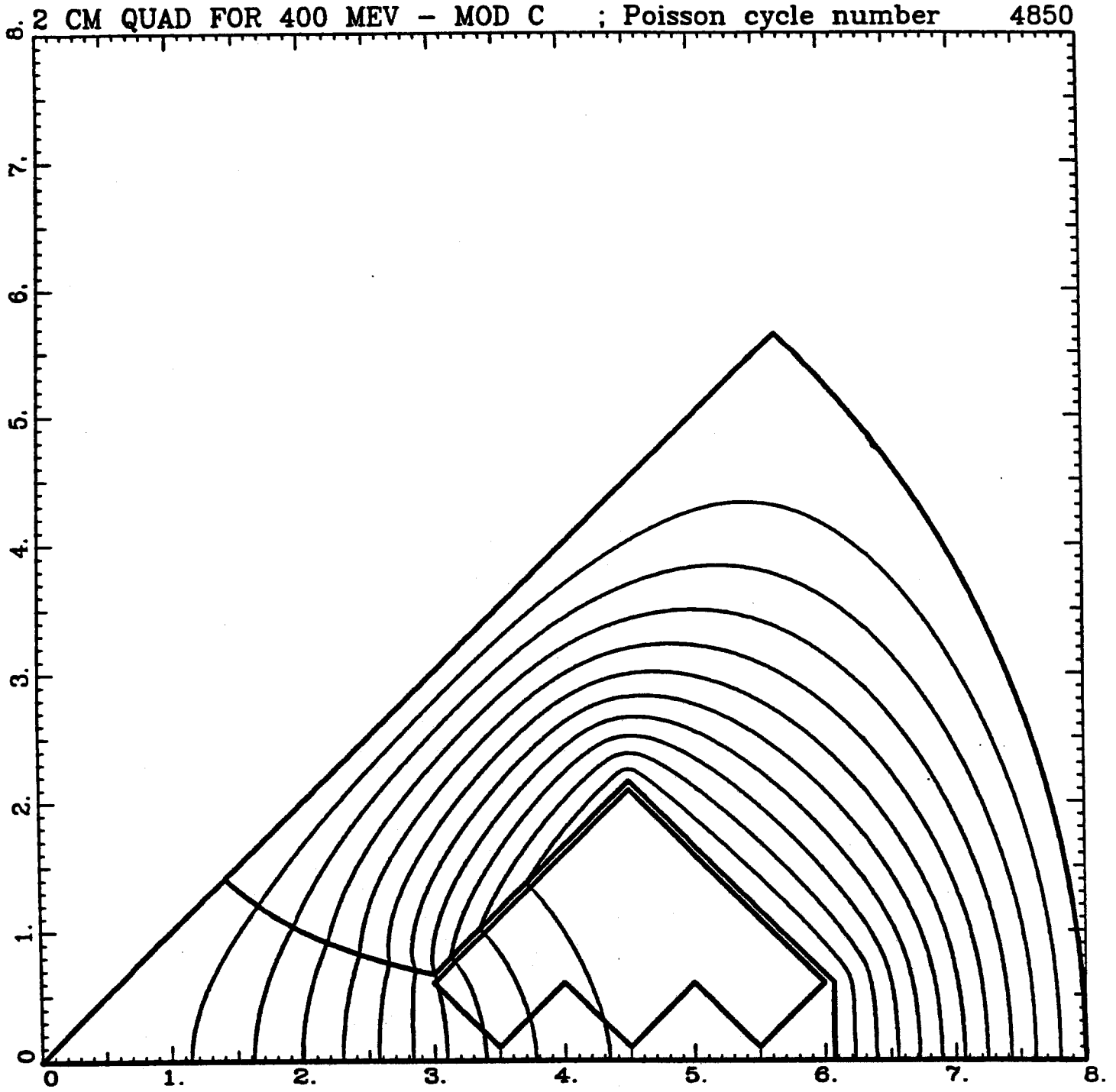

Figure 8: One octant in crossection of an 8 cm quadrupole with 2 cm bore radius

Aperture radius (r_p)	0.02	m
Magnetic length (l_{eff})	0.08	m
Maximum required gradient (B'_{max})	264.	kG/m
Number of turns per pole	12	
Current for B'_{max} (I_{max})	350.	A
Resistance (R)	2.1	mΩ
Inductance, parallel connection (L)	32.9	μH
Pulse length	~1.	ms
Peak voltage (V_{max})	~150.	V
Duty factor	1.5	%
Peak real power ($\hat{P}$)	812.	W
Average power ($\bar{P}$)	12.	W
Gradient error at 1.5 cm	<1.	%

Table 6: Properties of an Electromagnetic Quadrupole for $\frac{1}{2}\beta\lambda$ Couplers

Alvarez linac is ~ 67 cm; the first focusing unit in the new linac will be at least twice that. Longitudinal matching is obtained by allowing the bunches to oscillate in a bucket that provides longitudinal focusing at the geometric mean between that of the old and the new linacs for one quarter of an oscillation period,[12] a "bunch rotation". Therefore, if the beam exiting tank 5 is matched to its bucket and if the gradients in both machines are nominal, there is a unique length and gradient for a non-accelerating rf tank which produce the desired rotation and final bunch width. The rotation is conviently carried out at 800 MHz; in this case about fifty cells at ~ .7 MV/m are required. To match gracefully in the transverse plane it would be best to segment this rf structure into lengths intermediate between the upstream and downstream focusing cell lengths. However, on the basis of providing just enough quads to match β and α in both planes, the sections in the transition section are as long as, or even longer than, the first sections in the new linac. Thus, one can anticipate rather irregular beam envelope functions in the transition section; because the rf gradient is rather low, it is reasonable to consider larger quad and rf structure bore in this region to provide for extreme matching conditions.

The precise values for the longitudinal matching can not be known before comissioning and once known they can not be expected to remain completely fixed. Therefore, it must be possible to have the effect of an adjustment of both gradient and length of the matching tank. This effect is obtained by dividing the power feed into at least two independently adjustable parts. Independent adjustment of the gradients permits achieving the 90 deg bunch rotation with a range of available bunch widths. Figures 9 and 10 show beam envelopes in three

[12] This formulation of the matching condition is due to Fred Mills, priv. comm.

Quad	DAW $\beta_x = 2.1$; $\beta_y = 7.4$; $\alpha_x = \alpha_y = 0.$	SCC $\beta_x = \beta_y = 4.4$; $\alpha_x = -\alpha_y = 10.$
1	-7.40	-0.01
2	14.58	3.87
3	-17.80	-39.99
4	17.48	47.66
5	-16.55	43.42

Table 7: Quad strengths B'l [kG] in the Transition Section for DAW and SCC Linacs

dimensions for two different realisations of the matching scheme. The first is a four-section FODO arrangement which is appropriate for the six-section FODO modules favored in the preceding sections. The second version embodies doublet cells and is better for matching to doublets in the new linac. The component values recorded in Table 7 have been chosen to match from the initial conditions of Table 1 to the FODO and doublet focusing schemes applied above to the DAW and SCC parameters respectively.

8 Summary

This note attempts to summarise the present status of the overall design of the Tevatron Upgrade linac with respect to rf structure, focusing scheme, and matching to the existing linac. A general layout consisting of seven modules of disk-and-washer rf structure segmented into six sections of FODO transverse focusing has been described in some detail. The parameters of all major components have been specified. Several alternatives and variants which appear less desirable from available measurements and calculations have been mentioned to indicate the kind and extent of response that could be required if our present uncertainties are resolved contrary to expectation. This snapshot of work in progress can be expected in any case to be refined as measurements and design efforts on subsystems are focused into a more comprehensive and explicit conceptual design.[13] The purpose of this note is to promote that focus and to provide an informal discussion of some the remaining uncertainties and options.

[13] A new edition of the Conceptual Design Report is expected January, 1988.

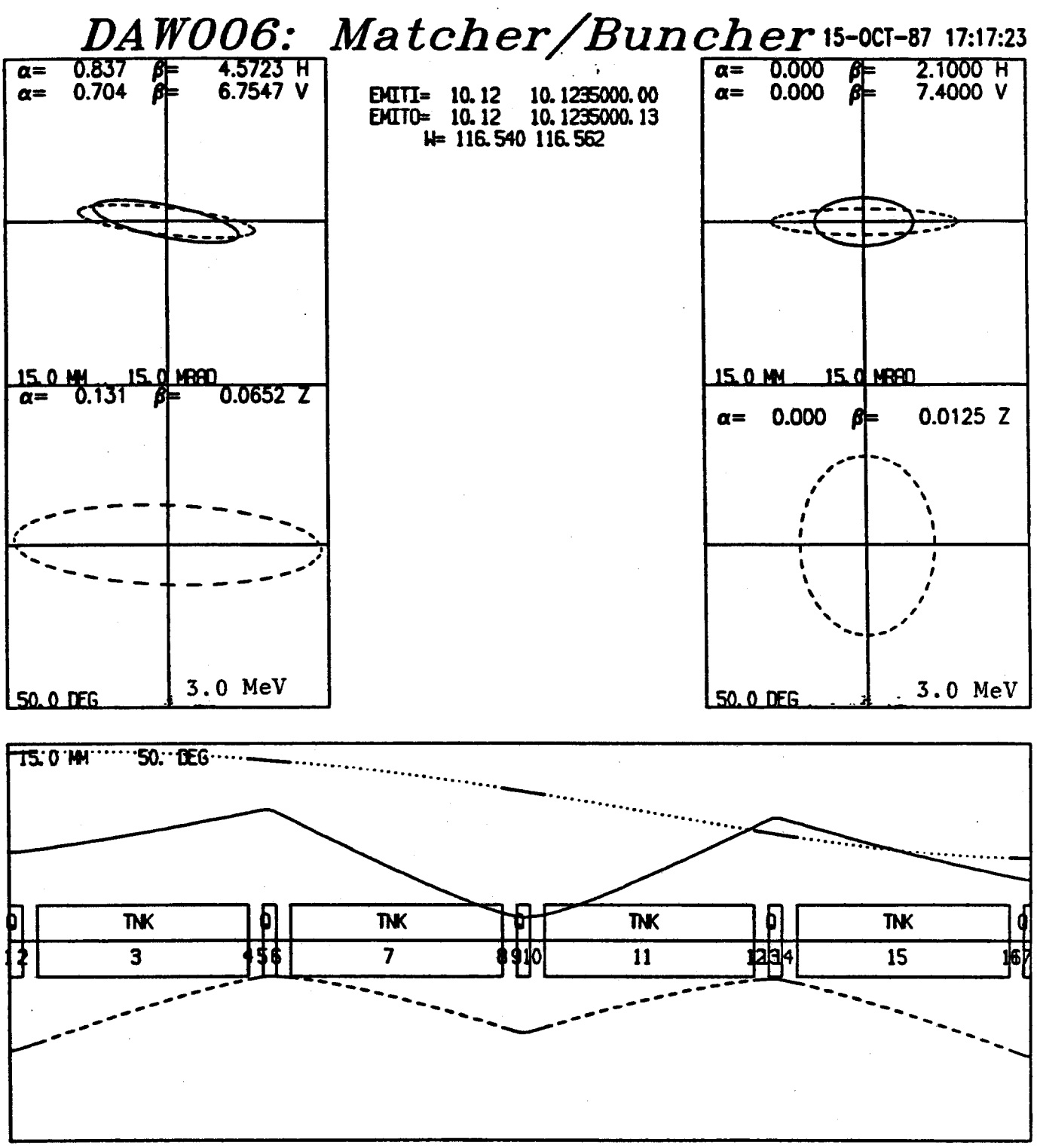

Figure 9: Beam envelopes in the transition section to the DAW FODO-focused Linac

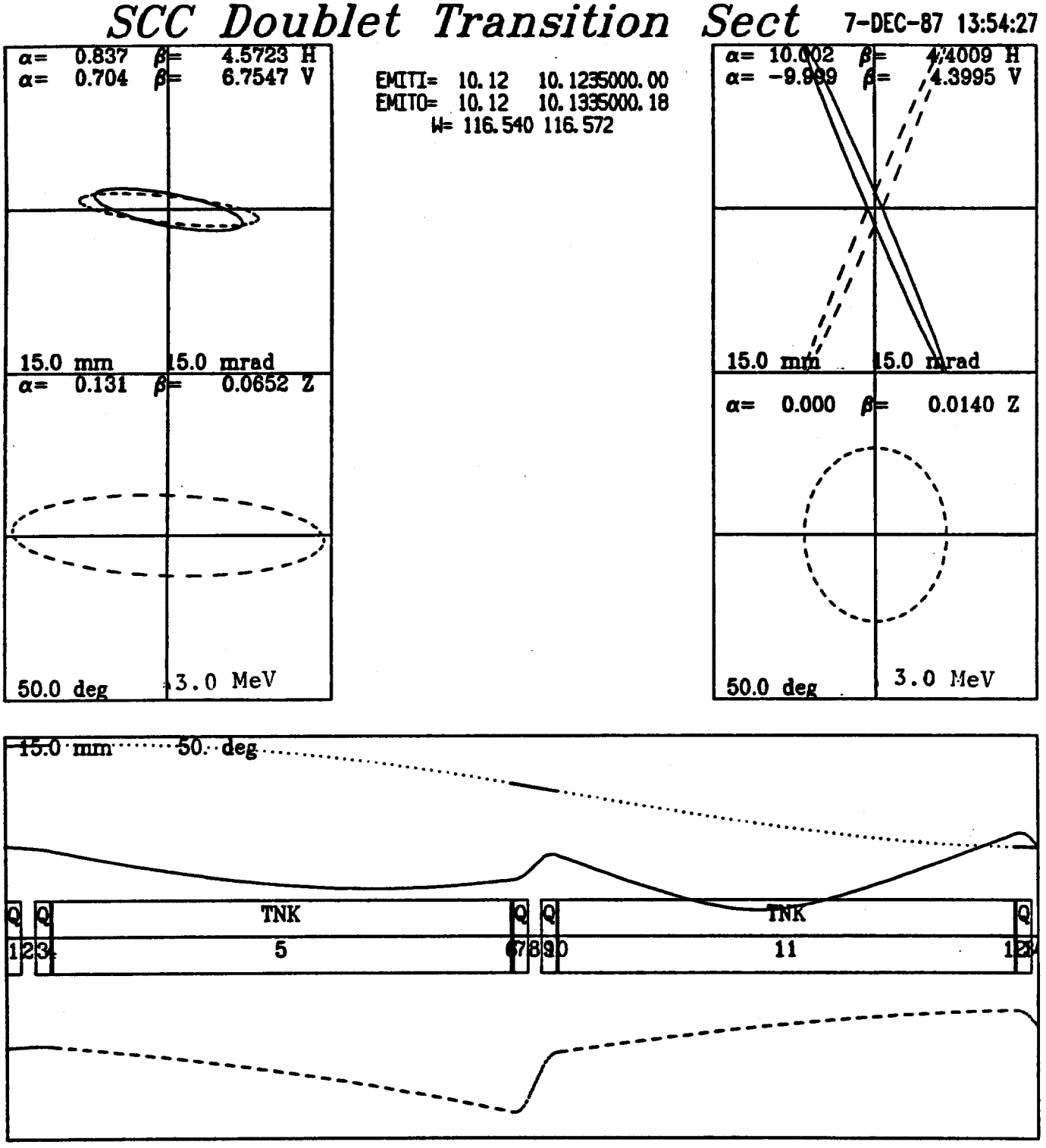

Figure 10: Beam envelopes in the transition section to the SCC Doublet-focussed Linac

References

[1] *Tevatron Upgrade – Linac Conceptual Design*, Fermilab(4/87)

[2] E. A. Knapp *et al.*, Rev. Sci. Inst., 39 no. 7(7/68)

[3] R. K. Cooper *et al.*, Radio-Frequency Structure Development for the Los Alamos/NBS Racetrack Microtron, LA-UR-83-95, Los Alamos Nat'l Lab.(1/83)

[4] W. D. Kilpatrick, Rev. Sci. Inst. 28,824(1957)